Experimental report

13/06/2019

Proposal: **4-03-1729** **Council:** 4/2017

Title: Quanturn Criticality in Iron DopedMnSi: A Neutron Spin Echo Study

Research area: Physics

This proposal is a resubmission of 4-03-1728

Main proposer: **Frank WEBER**

Experimental team: Lars Johannes BANNENBERG
Catherine PAPPAS
Frank WEBER

Local contacts: Peter FOUQUET
Peter FALUS

Samples: $Mn_{0.9}Fe_{0.1}Si$
$Mn_{0.92}Fe_{0.08}Si$

Instrument	Requested days	Allocated days	From	To
IN11	6	6	29/03/2018	04/04/2018

Abstract:

In recent years complex forms of magnetic order based on spin chirality in non-centrosymmetric systems has attracted great interest in condensed matter physics. Among many systems, MnSi is ideally suited to study the properties of unconventional magnetic states. With the proposed experiment we would like to extend our studies to Mn(1-x)Fe(x)Si, close to the quantum critical point, where the magnetic phase transition is suppressed to zero temperature. The high resolution neutron spin echo and polarization analysis capabilities of IN11 will allow us to investigate the interplay between the quantum critical point and the chiral fluctuations to establish the generality of the precursor phenomena and the effect of disorder on the helical magnetic order.

The archetype chiral magnet MnSi exhibits helical order with a spontaneous ordered moment of 0.45 μB/Mn and a long-wavelength (ℓ~18 nm) modulation of the spin structure that is pinned along the ⟨111⟩ crystallographic directions. The ordering temperature T_C is reduced with increasing pressure from ~ 29 K at ambient pressure to zero at a pressure of 14.6 kbar, where an unconventional non-Fermi liquid state sets-in [2]. Chemical pressure in the form of Fe doping in $Mn_{1-x}Fe_xSi$ reduces the ordering temperature [3-6] and possibly leads to two Quantum Critical Points: one located at x ≈ 0.11, where the long range magnetic order is suppressed and a second one at x ≈ 0.24, where the short magnetic order is suppressed as well. In particular, magnetic susceptibility and electric transport phenomena report a non-Fermi liquid behavior attributed to a chiral spin liquid state, which for x ≈ 0.108 should appear below 9 K [5]. In this system, our magnetization, susceptibility and SANS investigations led to the phase diagram shown in Fig. 1, where two characteristic concentrations have been identified: $x^* \approx 0.11$, above which the long range helimagnetic periodicity disappears and $x_C \approx 0.17$, where T_C vanishes [7].
The goal of the IN11 experiment was to investigate the influence of doping on the helimagnetic fluctuations and the phase transition. For this purpose we chose to investigate three single crystals, which were previously characterized by SANS [7], and have compositions close to x^* and x_C,: $Mn_{0.91}Fe_{0.09}Si$, $Mn_{0.89}Fe_{0.11}Si$ and $Mn_{0.86}Fe_{0.14}Si$. For these experiment the IN11 instrument was set in the paramagnetic NSE configuration and the incoming wavelength was 0.55 nm. As the helimagnetic pitch varies strongly with doping [3-7], the measurements were performed at different Q's for each sample. These were determined from the respective maxima of the magnetic scattering intensity, S(Q). We found Q=2π/ ℓ =0.58, 0.68 and 0.88 nm^{-1}, which correspond to ℓ=10.8, 9.2 and 7.1 nm, for x=0.09, 0.11 and 0.14 respectively. These values are in good agreement with our SANS results [7] and the literature [3-4].
Polarization analysis is an important constituent of the paramagnetic NSE measurement procedure and leads to a separation of the magnetic from the non-magnetic (background) contributions. This was done very accurately on IN11 due to the high flipping ratio and the excellent neutron flux of the instrument. Furthermore, it was possible to directly determine the chirality of themagnetic correlations [8]. The results for the temperature dependence of the helimagnetic scattering and the degree of left chirality are shown respectively in Fig. 2 and 3 for all three samples.
For x =0.09, the behavior bears strong similarities to that of the parent compound MnSi [8]. A jump of the intensity marks the first order phase transition at T_C=7.8±0.1 K and the scattering reflects full left-handed chirality not only in the ordered phase but also well above T_C. The magnetic scattering is completely chiral up to ~10 K, i.e up to ~T_C+2 K, a temperature interval significantly larger than in MnSi, where this behavior is seen only up to ~T_C+1 K.
The behavior for x =0.11 and 0.14, i.e. for $x^* < x < x_C$, changes dramatically as the evolution of the intensity with temperature is gradual without the jump of intensity at T_C. This is in agreement with our previous results [7]. Nevertheless, the left-handed chirality persists for x =0.11, for which composition the scattering is completely chiral below ~5K. However, if the doping is further increased, for x=0.14, this is no longer the case as the scattering is nearly achiral with a slight tendency for right handed chirality. Furthermore, at this composition, the chirality varies with Q.
On one side, these results confirm the disappearance of the helical Bragg peaks, and consequently of the long-range helical periodicity, for $x > x^*$ already reported in [7]. On the other side, they reveal that the evolution of the helimagnetic correlations with Fe doping is more complex than assumed so far. When the Fe concentration approaches x_C from below, the chirality changes and is even lost, a result that reflects competition between domains with opposite chirality.
In contrast to the results discussed so far, the NSE spectra, i.e. the intermediate scattering function, of the three samples, shown in Fig.4, do not disclose any dramatic change with doping. The relaxation is exponential and the low temperature spectra are completely elastic, not only for x =0.09 but also x =0.11 and 0.14. This result excludes the existence of a spin liquid ground state for $x > x^*$. A closer inspection of the results shown in Fig. 4 reveals an evolution of the relaxation with temperature that is fastest for x =0.09 and slowest for x =0.14, and thus follows the evolution

of the intensity shown in Fig. 2 and of the correlation length discussed in [7].
Due to experimental issues at the end of experiment Nr. 4-03-1729 the measurements on the 14% sample were finalized in September 2018 during the TEST-2952 beam time.

References

[1] A. Bauer, C. Pfleiderer, in *Topological Structures in Ferroic Materials* **228,** 1–28 (Springer International Publishing, 2016);

[2] C. Pfleiderer *et al.*, Nature **427** (2004).

[3] A. Bauer, *et al. Phys. Rev. B* **82,** 064404 (2010);

[4] S.V. Grigoriev *et al. Phys. Rev. B* **83,** 224411 (2011);

[5] S.V. Demishev *et al. Jetp Lett.* **100,** 28–31 (2014) and S.V. Demishev et al, Jetp Lett. 103, 321–327 (2016);

[6] C. Franz, *et al.. Phys. Rev. Lett.* **112,** 186601 (2014)

[7] L.J. Bannenberg *et al., Phys. Rev. B* ***98,*** 184430 and 184431 (2018);

[8] C. Pappas *et al*., *Phys. Rev. Lett* **102** (2009) and *Phys. Rev. B* **83** 224405 (2011).

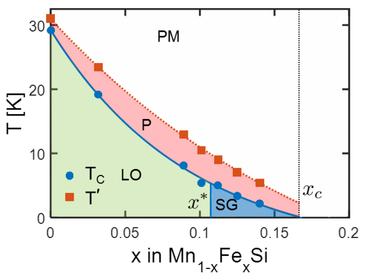

Fig.1: Phase diagram of $Mn_{1-x}Fe_xSi$ deduced from SANS and susceptibility measurements [7]. T_C is the transition temperature. T' marks the onset of short-ranged and fluctuating helimagnetic correlations characteristic of the precursor phase.

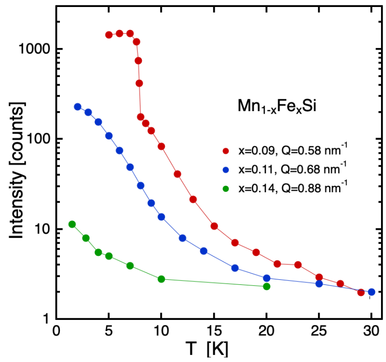

Fig.2: Temperature dependence of the helimagnetic scattering intensity for the three samples measured at the maximum of S(Q), i.e. at the Q-values that correspond to the respective helimagnetic pitch.

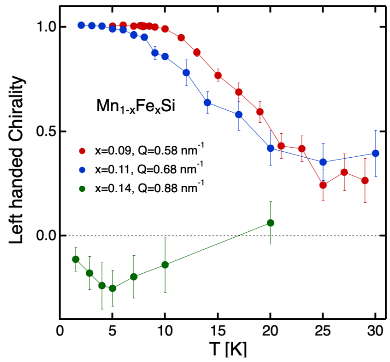

Fig.3: Temperature dependence of the chiral fraction of the scattering measured at the maximum of S(Q), i.e. at the Q-values that correspond to the respective helimagnetic pitch.

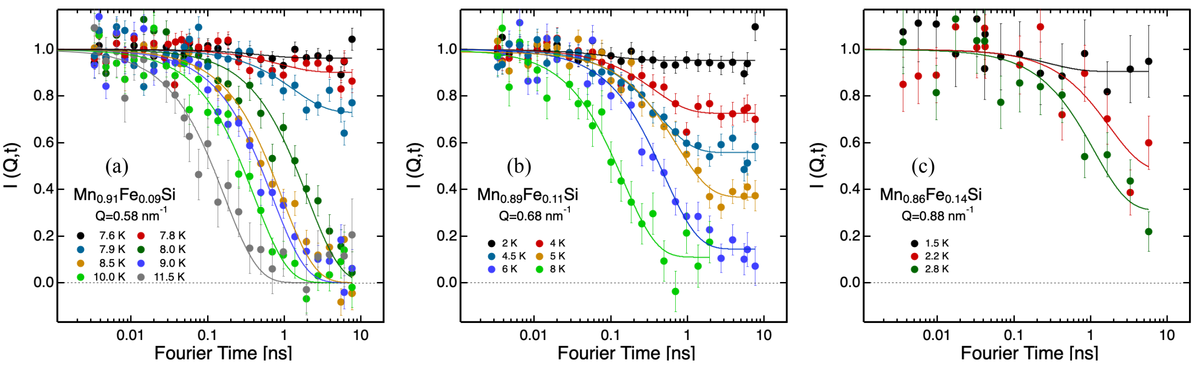

Fig.4: Intermediate scattering function, reflecting the dynamic correlations at the respective values of Q, which correspond to the respective periodicity of the helimagnetic correlations, for $Mn_{0.91}Fe_{0.09}Si$ (a), $Mn_{0.89}Fe_{0.11}Si$ (b) and $Mn_{0.86}Fe_{0.14}Si$ (c). The lines represent fits to an exponential decay.